Phase Changes in Ge Nanoparticles

Hsiang Wei Chiu, Christopher N. Chervin, and Susan M. Kauzlarich*

Department of Chemistry, University of California Davis, One Shields Avenue, Davis, California 95616

Received March 29, 2005. Revised Manuscript Received May 20, 2005

Butyl-capped crystalline germanium (Ge) nanoparticles were synthesized at room temperature in dimethoxyethane by reduction of $GeCl_4$ with Na(naphthalide) and subsequent reaction with butyl Grignard. The nanoparticles were isolated in hexane and characterized by transmission electron microscopy (TEM), selected area electron diffraction (SAED), energy-dispersive X-ray spectroscopy (EDX), elemental analysis, and X-ray powder diffraction (XRD). The product from this room-temperature reaction was heated under vacuum at temperatures of 200−600 °C at 50 °C intervals. The product obtained from the 300 °C treatment was soluble in hexane, while the products from temperatures greater than 300 °C were not. SAED was consistent with crystalline Ge from the initial synthesis at room temperature and amorphous Ge for the product heated under vacuum to 300 °C. X-ray powder diffraction of the 300 °C product shows the transition from amorphous to crystalline nanoparticles occurring between 550 and 600 °C. TEM shows that the nanoparticles remain dispersed and nonaggregated up to 600 °C. Differential scanning calorimetry (DSC) shows a crystallization exotherm at 561 °C and a melting endotherm at 925 °C for nanoparticles with average diameter of 8 nm.

Introduction

In the history of solar cells and satellite arrays, germanium has been an important component in the preparation of solar cells.[1−3] Gallium arsenide (GaAs) cells have been available since the 1960s and have been much improved to make high-efficiency photovoltaics.[4] It has been found that high-efficiency photovoltaics can be made by using germanium as a substrate for GaAs cell.[5,6] Germanium is lattice-matched to GaAs and it is less expensive than GaAs. Ge is also stronger and more robust than GaAs; hence, the cells can be made on thinner substrates. Thinner substrates translate into a lighter, high-efficiency cell using less GaAs than ones without Ge. A current challenge is the production of large-area, low-cost, flexible GaAs photovoltaic cells. With the rise of nanotechnology, it is envisioned that a lightweight, flexible photovoltaic may be constructed from nanoparticles.[7,8] Quantum dots offer the option of one material with different band gap energies. An alternate use of nanoparticles (NPs) is as a soluble form of precursor that could be deposited as a thin film using ink-jet or laser printing technologies.[9] This would also require that the film could be made into a single-crystal substrate and that the NPs be compatible with printing technology. This idea has been demonstrated for metal NPs and holds promise for other types of NPs.[9] The use of NPs may enable low-cost fabrication of lightweight photovoltaic cells while keeping their high-energy conversion capabilities.

There have been several recent reports of the production of Ge NPs prepared from the reduction of $GeCl_4$ under moderate or ambient conditions.[10−13] These NPs are initially terminated with either −Cl or −H and then terminated with an organic ligand. The particles produced show a fairly narrow size distribution and photoluminescence. Similar results have also been obtained for Ge NPs produced from supercritical reactions[14,15] and there has been some speculation concerning the origin of the photoluminescence.[15] This group has investigated several routes to the production of group IV NPs.[16−19] There is an early report that the reduction route leads to amorphous group IV NPs.[20] In an interest to

(1) McConnell, R. D. *Future Generation Photovoltaic Technologies*; American Institute of Physics: Woodbury, NY, 1997; Vol. 404.
(2) Marti, A.; Luque, A. *Next Generation Photovoltaics*; Institute of Physics Publishing: Bristol, UK, 2004.
(3) Bailey, S. G.; Flood, D. J. *Prog. Photovoltaics* **1998**, *6*, 1−14.
(4) Hardingham, C.; Wood, S. P. *GEC Rev.* **1998**, *13*, 163−171.
(5) Blondeel, A.; Clauws, P.; Depuydt, B. *Mater. Sci. Semicond. Process.* **2001**, *4*, 301−303.
(6) Mauk, M. G.; Balliet, J. R.; Feyock, B. W. *J. Cryst. Growth* **2003**, *250*, 50−56.
(7) Bukowski, T. J.; Simmons, J. H. *Crit. Rev. Solid State Mater. Sci.* **2002**, *27*, 119−142.
(8) Valeev, R. G.; Deev, A. N.; Ruts, Y. V. *Surf. Interface Anal.* **2004**, *36*, 955−958.
(9) Huang, D.; Liao, F.; Molesa, S.; Redinger, D.; Subramanian, V. *J. Electrochem. Soc.* **2003**, *150*, G412−G417.
(10) Wilcoxon, J. P.; Provencio, P. P.; Samara, G. A. *Phys. Rev. B: Condens. Matter* **2001**, *64*, 035417−035419.
(11) Hope-Weeks, L. J. *Chem. Commun.* **2003**, 2980−2981.
(12) Fok, E.; Shih, M.; Meldrum, A.; Veinot, G. C. *Chem. Commun.* **2004**, 386-387.
(13) Gerung, H.; Bunge, S. D.; Boyle, T. J.; Brinker, C. J.; Han, S. M. *Chem. Commun.* **2005**, 1914−1916.
(14) Lu, X.; Ziegler, K. J.; Ghezelbash, A.; Johnston, K. P.; Korgel, B. A. *Nano Lett.* **2004**, *4*, 969−974.
(15) Gerion, D.; Zaitseva, N.; Saw, C.; Casula, M. F.; Fakra, S.; Van Buuren, T.; Galli, G. *Nano Lett.* **2004**, *4*, 597−602.
(16) Taylor, B. R.; Kauzlarich, S. M.; Lee, H. W. H.; Delgado, G. R. *Chem. Mater.* **1998**, *10*, 22−24.
(17) Taylor, B. R.; Kauzlarich, S. M.; Delgado, G. R.; Lee, H. W. H. *Chem. Mater.* **1999**, *11*, 2493−2500.
(18) Taylor, B. R.; Fox, G. A.; Hope-Weeks, L. J.; Maxwell, R. S.; Kauzlarich, S. M.; Lee, H. W. H. *Mater. Sci. Eng. B* **2002**, *96*, 90−93.
(19) Tanke, R. S.; Kauzlarich, S. M.; Patten, T. E.; Pettigrew, K. A.; Murphy, D. L.; Thompson, M. E.; Lee, H. W. H. *Chem. Mater.* **2003**, *15*, 1682−1689.
(20) Kornowski, A.; Giersig, M.; Vogel, R.; Chemseddine, A.; Weller, H. *Adv. Mater.* **1993**, *5*, 634−636.

10.1021/cm050674e CCC: $30.25
Published on Web 08/17/2005

gain an understanding of the product obtained from the ambient reduction route, butyl-terminated Ge NPs have been produced by the reduction of $GeCl_4$ with Na naphthalenide. These NPs were further reacted with a Grignard reagent to produce alkyl-terminated NPs. This product shows small polydispersity (~10%) and electron diffraction consistent with crystalline Ge. Elemental analysis is consistent with the product being a mixture of Ge NPs and hydrocarbon. Heating this product under vacuum to various temperatures shows that this material undergoes a transition to amorphous (or paracrystalline[21]) NPs by 300 °C and can be converted back to crystalline NPs by 561 °C. In situ X-ray powder diffraction, along with TEM, SAED, and calorimetry, studies will be presented.

Experimental Section

Materials. Ethylene glycol dimethyl ether (glyme) (Acros, 99+%) was dried and distilled twice from a Na−K alloy under argon. The sodium−potassium (Na−K) alloy was freshly prepared from a mixture of sodium (Aldrich, 99%) and potassium pieces (Aldrich, 98%). Naphthalene ($C_{10}H_8$) (Fisher, refined, 99.98%), germanium tetrachloride, ($GeCl_4$) (Acros, 99.99%), and butylmagnesium chloride (Aldrich, 2 M) were used without further purification. HPLC grade water (EM Science) and HPLC grade hexane (Aldrich) were used as received. Manipulations of these chemicals were handled either in a N_2-filled glovebox or on a Schlenk line using standard anaerobic and anhydrous techniques.

Sodium Naphthalenide (Na(naphth)) Synthesis. Na metal (0.5190 g,0.02258 mol) was added to a Schlenk flask in a drybox and transferred to a Schlenk line. Then 2.894 g (0.02258 mol) of naphthalene was added under Ar. Approximately 70 mL of freshly distilled and degassed glyme was added to the solids and the mixture was stirred overnight. Upon dissolution of the Na metal, the solution changed from colorless to a dark green color.

Germanium Nanoparticle Synthesis. A 70 mL solution of Na(naphth) was added rapidly via cannula to 0.70 mL (0.00602 mol) of $GeCl_4$ in 300 mL of glyme in a Schlenk flask at room temperature. The solution immediately changed from a clear to a black suspension upon the addition of the Na(naphth) mixture. After 10 min of stirring, the suspension was allowed to settle. Once settled, there was a dark black solid at the bottom of the flask and a dark yellow solution on the top. The orange solution was vacuum-dried to remove the naphthalene. Freshly distilled and degassed glyme (250 mL) was then added to the flask, followed by 3.01 mL (0.00602 mol) of *n*-BuMgCl. The mixture was left to stir for 12 h. The mixture was pumped down to dryness, the NPs were extracted with hexane, and the extract was rinsed with acidified water. After the removal of hexane in vacuo, with mild heating, ca. 500 mg of viscous orange oil was obtained. The elemental analysis of the orange oil, as-prepared Ge NPs were $Ge(C_4H_9)_{2.3}$. Calculated: Ge, 35.60; C, 54.17; H, 10.23. Found: Ge, 31.56; C, 56.13; H, 9.1; Cl, 0.67; Na, 0.57; Mg, 0.03.

Heat Treatment. The as-prepared Ge NPs were loaded into an alumina boat which was then placed into a quartz tube. The tube was attached to a high-vacuum apparatus and was inserted into a temperature-controlled furnace. The sample was brought up to a targeted temperature under vacuum conditions with a heating scheme of 1 °C/min to 90 °C, dwell for 3 h, 1 °C/min to the desired temperature, then dwell for 12 h. The final temperatures were 200, 250, 280, 300, 320, 360, 400, 420, and 450 °C. For temperatures above 300 °C the products were black solids. An orange solid was produced at 300 °C and below 300 °C orange oil remained. All the black solids were insoluble in any common nonpolar and polar solvents. The 300 °C products along with the products obtained at temperatures lower than 300 °C were soluble in hexane. The elemental analysis of the orange solid after heating to 300 °C, $Ge(C_4H_9)_{0.75}$. Calculated: Ge, 55.98; C, 27.77; H, 5.24. Found: Ge, 58.04; C, 29.23; H, 5.4; Cl, <0.02; Na, <0.05; Mg, <0.05%. The yellow oil from the 300 °C heating was also characterized by UV−vis, photoluminescence, elemental analysis, and TEM. The elemental analysis total was low for the yellow oil. Assuming that this is due to inclusion of glyme in the oil, oxygen was assumed to be the missing component. The elemental analysis of the yellow oil, $Ge(C_{3.25}H_{6.59}O)_7$. Calculated: Ge, 14.40; C, 54.15; H, 9.23. Found: Ge, 14.42; C, 54.04; H, 9.21; Cl, 0.36; Na, <0.05; Mg, <0.05%. The C:H ratio is approximately 1:2, but no simple formula which included oxygen in an integral ratio could be deduced. Elemental analysis was also obtained for a black powder sample prepared by heating under vacuum at 400 °C. This sample was also used for the TGA/DSC measurement. The elemental analysis of the black solid, $Ge(C_4H_9)_{0.15}$. Calculated: Ge, 89.44; C, 8.88; H, 1.68. Found: Ge, 82.47; C, 8.27; H, 1.88; Cl, <0.02; Na, <0.005; Mg, <0.005%.

X-ray Powder Diffraction. Powder X-ray diffraction (XRD) data were collected on an Inel-CPS120 diffractometer using Cu Kα radiation. The high-temperature XRD (HTXRD) measurements were performed in flowing argon with a heating rate of 1 °C/min and a collection time of 30 min. Data were collected in an interval of 50−600 °C. Error in temperature measurements was estimated not to exceed ±10 °C. For room-temperature XRD measurements, samples were placed on a zero background quartz plate. Ge powder (Acros, 99.99%) was used to determine the instrument width.

Characterization. Transmission electron microscopy (TEM) and energy-dispersive X-ray (EDX) spectroscopy analyses of these NPs were performed on a Philips CM-12, operating at 100 keV. TEM samples were prepared by dipping the holey, carbon-coated, 400-mesh electron microscope grid into the hexane colloid, followed by heating in a 120 °C oven overnight. Chemical analysis was obtained from Desert Analytics Laboratory in Tucson, AZ. UV−vis spectra were obtained with a HP 8452A diode array spectrophotometer. Photoluminescence spectra of hexane solutions were measured on a Jobin Yvon Horiba FluoroMax-P luminescence spectrophotometer. HPLC grade hexane was used as a blank solution prior to recording each sample. Thermogravimetric analysis (TGA) and differential scanning calorimetry (DSC) were performed simultaneously with a Netzsch 449 Thermal Analyzer in the temperature range of 25−1000 °C under a flowing argon atmosphere and using a 10 °C/min ramping scheme. About 25 mg of the black powder obtained from a sample heated to 400 °C under vacuum was used. Ge powder (Across, 99.99%) was also measured under identical conditions.

Results and Discussion

The as-prepared Ge NPs produced from this reaction were isolated as an orange oily product and found to be soluble in nonpolar solvents, such as hexane. Elemental analysis showed a significant amount of hydrocarbon giving the relative stoichiometry of $Ge(C_4H_9)_{2.3}$. To obtain a dry powder, the sample was heated under vacuum to various temperatures. At temperatures lower than 300 °C, the product remained an oily substance. As the product was heated, yellow oil was removed, and by 300 °C, a dry orange powder was obtained. Elemental analysis of the orange powder was

(21) Treacy, M. M. J.; Gibson, J. M.; Keblinski, P. J. *J. Non-Cryst. Solids* **1998**, *231*, 99−110.

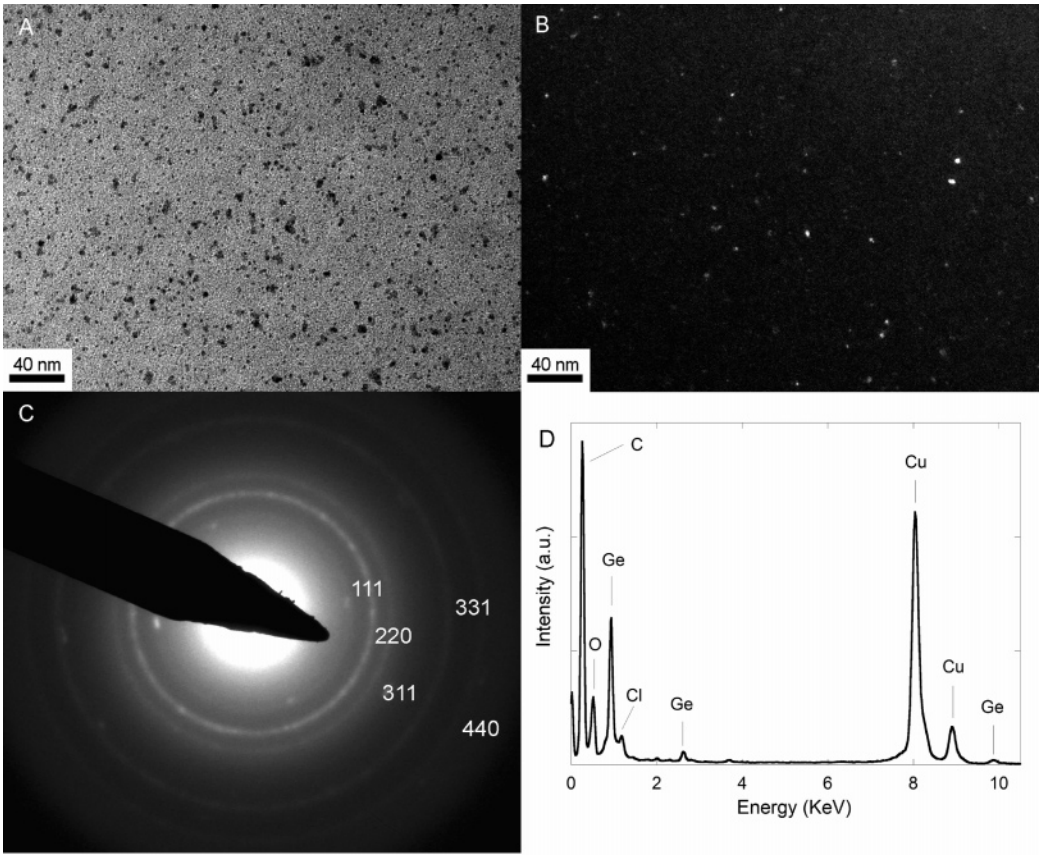

Figure 1. (A) Bright field TEM micrographs, (B) dark field TEM micrographs, (C) selected area diffraction, and (D) energy-dispersive X-ray spectrum of butyl-terminated Ge NP as-prepared.

Scheme 1

$$\underset{\text{Ge np, as prepared}}{Ge(C_4H_9)_{2.3}} \xrightarrow[\text{vacuum, } 300^oC]{} \underset{\text{orange powder}}{Ge(C_4H_9)_{0.75}} + \underset{\text{yellow oil}}{Ge(C_{3.25}H_{6.59}O)_7}$$

consistent with the stoichiometry $Ge(C_4H_9)_{0.75}$. The orange powder could be redispersed in all nonpolar hydrocarbon solvents similar to the as-prepared sample. The yellow oil also obtained from the 300 °C vacuum treatment was collected for elemental analysis and showed a smaller amount of Ge, suggestive of a Ge-containing polymeric side product. The elemental analysis total was low for this product and oxygen was assumed to be the missing element. The composition was consistent with the stoichiometry of $Ge(C_{3.25}H_{6.59}O)_7$. Scheme 1 outlines the heating of Ge NPs showing the compositions obtained from elemental analysis.

A yellow viscous liquid has also been isolated from high-pressure reactions.[15] It shows a strong blue-green luminescence under long wavelength illumination of a handheld UV lamp.[15] The yellow oil that we obtain from this room-temperature reaction shows strong blue-green luminescence. Presumably, we have obtained a similar product which is mixed with the Ge NPs produced by reduction under ambient conditions. It has been suggested that the amount of oil side product may be controlled by initial concentration and reaction conditions for the high-pressure reaction.[15] This may also be the case for the ambient condition reaction, and further investigation of the reaction products as a function of concentration is underway.

The final product was an insoluble dry black powder for all samples heated under vacuum to temperatures higher than 320 °C. The products obtained after heat treatment above 300 °C have been characterized by XRD, TEM, EDX, SAED, and TGA/DSC.

Figure 1 shows bright field and dark field images of the as-prepared sample. The bright field image shows that the NPs are well-dispersed. The dark field image shows bright spots indicative of scattering of the electrons according to Bragg's law.[22] Figure 1C is the electron diffraction image of an as-prepared sample. The rings were measured and are consistent with Ge {111}, {220}, {311}, {331}, and {440}. The size distribution of the as-prepared sample is 4.5 ± 1.1 nm for 1017 particles. In Figure 1D, EDX spectroscopy confirmed the presence of germanium. Chlorine is observed and attributed to a small amount of NaCl present and the presence of copper and oxygen is attributed to the grid. Carbon is also present, attributed to both the grid and the sample. The elemental analysis shows a significant amount of hydrocarbon and this as-prepared sample is an orange oily substance. The relationship between the numbers of Ge atoms in the NP versus the number of surface R groups has been calculated by using the density of bulk germanium, assuming a spherical shape with each surface Ge bonded to one R group. The composition for a 4 nm Ge NP terminated with R groups is estimated to have the stoichiometry $Ge_{1790}R_{308}$, based on density arguments and full surface coverage, and therefore the relative stoichiometry of $Ge(C_4H_9)_{0.17}$. This calculation indicates that this diameter particle would have significantly less hydrocarbon than what is observed in the

(22) Williams, D. B.; Carter, B. C. *Transmission Electron Microscopy*; Plenum Press: New York, 1996.

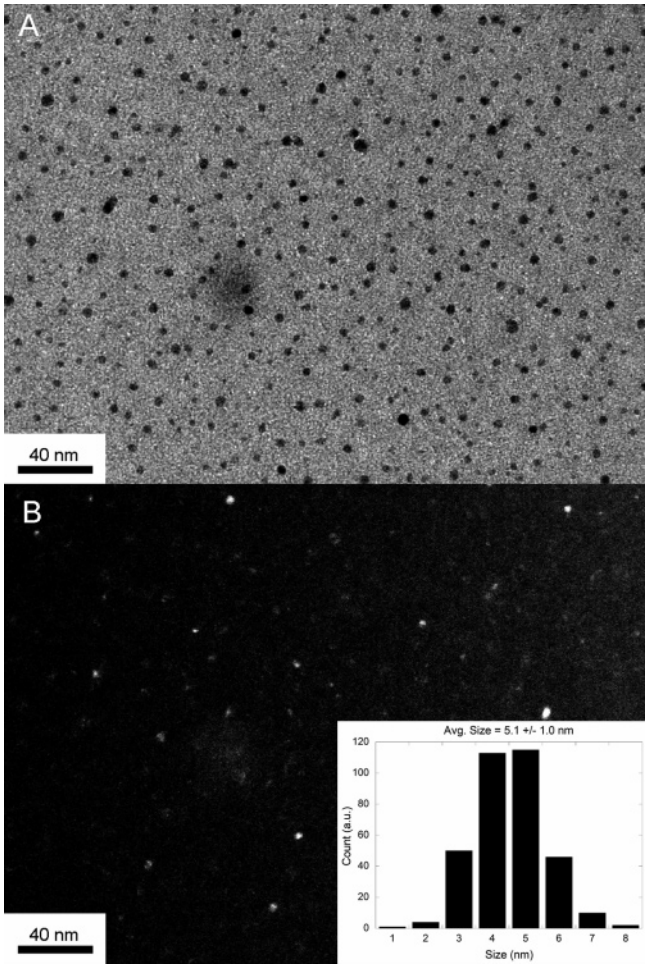

Figure 2. (A) Bright field and (B) dark field TEM micrographs of Ge NPs heated at 300 °C under vacuum. Inset shows the size distribution.

as-prepared sample, $Ge(C_4H_9)_{2.3}$, suggesting that the as-prepared sample is a mixture of NPs and side product.

Figure 2 shows the bright field and dark field images of orange powder obtained after heating to 300 °C under vacuum. The bright field image shows well-isolated NPs. The dark field image shows some bright spots; however, an SAED pattern could not be obtained. The inset provides the size distribution of this sample. The average diameter is 5.1 ± 1.0 nm based on counting 354 particles. This initial sample was prepared in a manner similar to that shown in Figure 2, but is not the same as-prepared sample. Small differences in average size are expected; however, all samples were prepared in a similar way at room temperature to make NPs approximately 4−5 nm in diameter. EDX spectroscopy is consistent with the presence of germanium. The elemental analysis of the 300 °C heated orange solid is $Ge(C_4H_9)_{0.75}$, where the hydrocarbon-to-Ge ratio is still too high for that predicted for 5 nm NPs, $Ge(C_4H_9)_{0.14}$, based on the calculated relative stoichiometry obtained using simple density and surface coverage approximations. The yellow oil was also investigated by TEM, but no NPs were found on the grid, suggesting that this material is an organic polymer. The yellow oil shows a total elemental analysis lower than 100 with the remaining amount assigned to oxygen. This may be due to a side reaction with the glyme solvent, giving the stoichiometry of $Ge(C_{3.25}H_{6.59}O)_7$. The yellow oil may be a

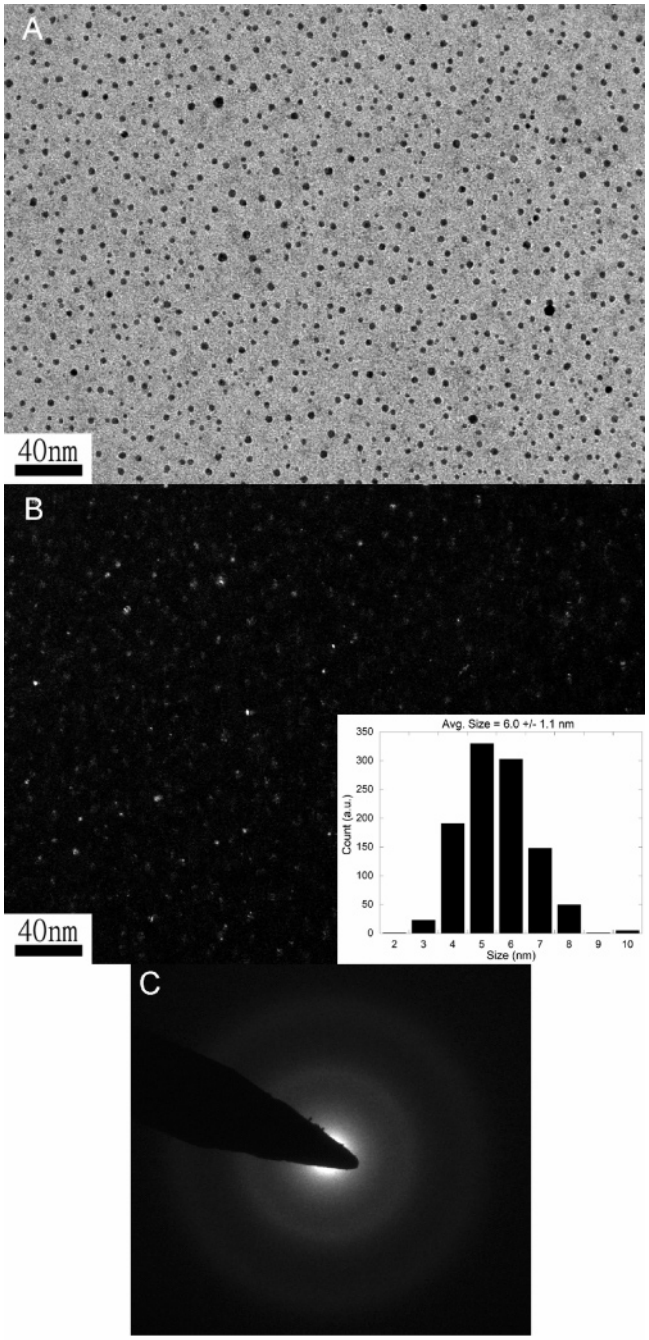

Figure 3. (A) Bright field TEM micrographs, (B) dark field TEM micrographs, and (C) selected area diffraction of Ge NPs heated to 450 °C under vacuum. Inset shows the size distribution of the sample.

Ge-containing polymer since the boiling point is 300 °C under vacuum. Further characterization of this luminescent material is underway.

Figure 3 shows the bright field and dark field images of Ge NPs that were heated to 450 °C under vacuum. The bright field image shows well-dispersed particles and the dark field image shows bright spots. The size distribution is provided as an inset and the average diameter is 6.0 ± 1.1 nm based on 1000 particles. SAED was performed, Figure 3C, and two diffused rings were observed, typical of amorphous Ge.[23] Amorphous Ge has been well-studied and crystal structure

(23) Edington, J. W. *Interpretation of transmission electron micrographs*; Macmillan: London, 1975.

has short range order that gives rise to two diffraction peaks.[24−28] EDX spectroscopy revealed the presence of germanium.

The most common techniques used to confirm crystallinity in TEM techniques are bright field and dark field imaging.[23] Dark field images are formed by using scattered electrons. Bright spots are seen in the dark field because they obey the Bragg condition. For highly crystalline materials, selected-area diffraction (SAED) can be performed on the material to confirm crystallinity. This is clearly the case for the as-prepared sample where both dark field and SAED confirm crystallinity. For the two samples heated at temperatures of 300 and 450 °C, dark field images show bright spots; however, SAED patterns consistent with crystalline Ge were not observed. Bright spots in dark field images have also been observed in microscopy studies on deposited amorphous Ge and were originally attributed to microcrystalline structure.[21,25] More recent work has shown that Si and Ge amorphous films can give rise to domains containing medium range order that diffracts electrons in the dark field image, but is not coherent for the SAED pattern.[21,25] This type of short or medium range order that provides dark field images but not electron diffraction patterns has been referred to as para-crystallinity.[21] This effect is apparent for the NPs obtained after being heated to between 300 and 500 °C under vacuum.

To more systematically explore the effect of heating, a Ge NP sample that was pretreated at 300 °C under vacuum was investigated by in situ X-ray diffraction while heating under flowing argon. This allowed for diffraction patterns to be obtained on the same initial sample at different temperatures. This is important in order to remove any effects that different average sized NPs may have had on the experiment and resulting electron microscopy measurements. Figure 4 shows diffraction patterns obtained at various temperatures. Two broad peaks are present in the X-ray diffraction patterns obtained between 100 and 400 °C, with maxima at approximately 28° and 50° 2θ, consistent with what is observed in SAED patterns. The broad diffraction peaks are consistent with the observation of bright spots in the dark field images showing medium range order, consistent with amorphous Ge. At 450 °C, sharp peaks assigned to the Al_2O_3 sample holder are observed due to shrinkage of the sample with heating. At 600 °C, the broad peaks are no longer present and new peaks corresponding to the four main Ge indices are observed: (111), 27.3°; (220), 45.4°; (311), 53.7°; and (400), 66.0°. These data support the postulate that the NPs are amorphous by X-ray diffraction (and SAED) for samples heated above 300 °C and that there is a phase change from amorphous to crystalline for the NPs between 500 and 600 °C.

Figure 5 shows the X-ray diffraction pattern at room temperature for the sample heated to 600 °C and the peaks

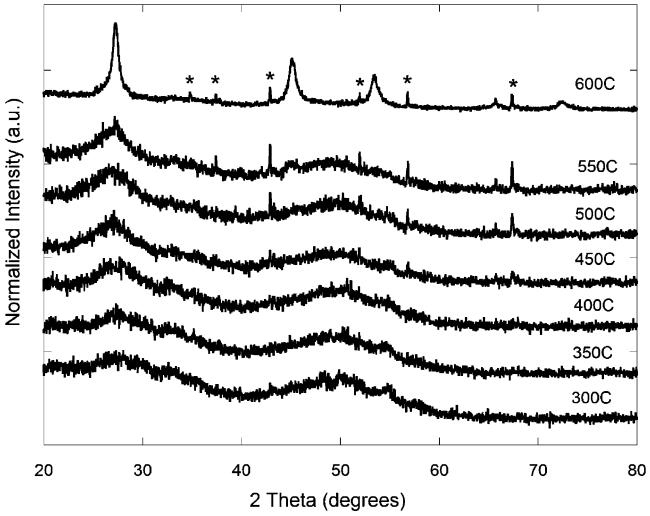

Figure 4. In situ temperature profile XRD of Ge NPs (heated under vacuum at 300 °C). Diffraction patterns were measured immediately after reaching each temperature. Additional peaks associated with the Al_2O_3 sample holder became apparent during shrinkage of the sample while heating and are marked with an *.

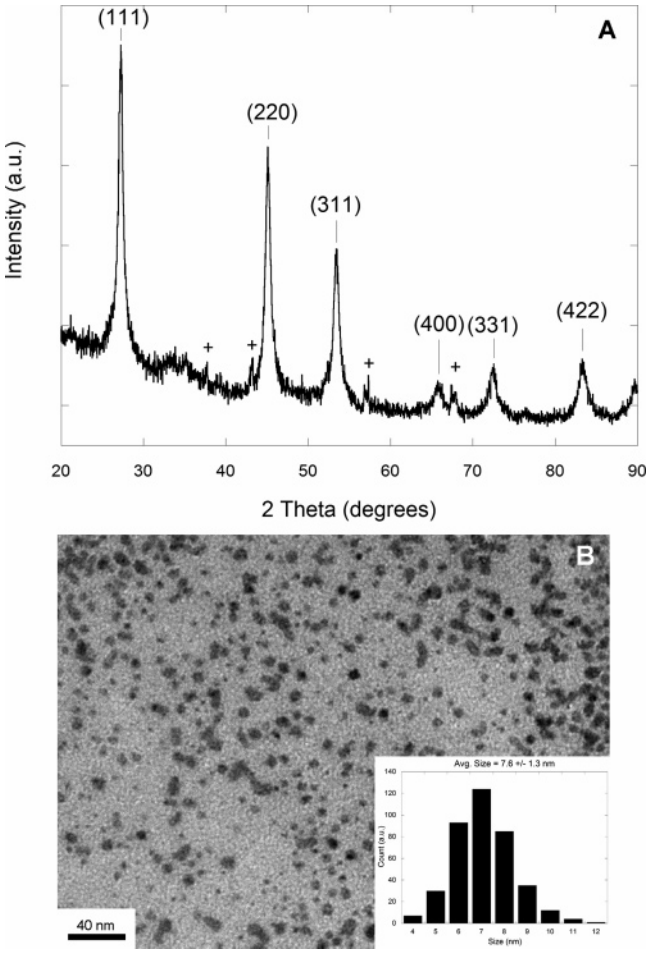

Figure 5. (A) Powder XRD pattern (+ signs correspond to the Al_2O_3 sample holder) and (B) bright field TEM micrograph of Ge NPs heated to 600 °C under vacuum. Inset shows the size distribution of the sample.

denoted by a + correspond to the alumina sample holder. With use of the Debye−Scherrer formula[29] for the Ge (111) diffraction peaks, the particle size is calculated to be 8.0 ±

(24) Etherington, G.; Wright, A. C.; Wenzel, J. T.; Dore, J. C.; Clarke, J. H.; Sinclair, R. N. *J. Non-Cryst. Solids* **1982**, *48*, 265−289.
(25) Gibson, J. M.; Treacy, M. M. J. *Phys. Rev. Lett.* **1997**, *78*, 1074−1977.
(26) Gibson, J. M.; Treacy, M. M. J.; Voyles, P. M. *Ultramicroscopy* **2000**, *83*, 169−178.
(27) Jamieson, J. C. *Science* **1963**, *139*, 762−764.
(28) Kasper, J. S.; Richards, S. M. *Acta Crystallogr.* **1964**, *17*, 752−755.
(29) Cullity, B. D. *Elements of X-ray Diffraction*; Addison-Wiley Publishing Company, Inc.: Reading, MA, 1978.

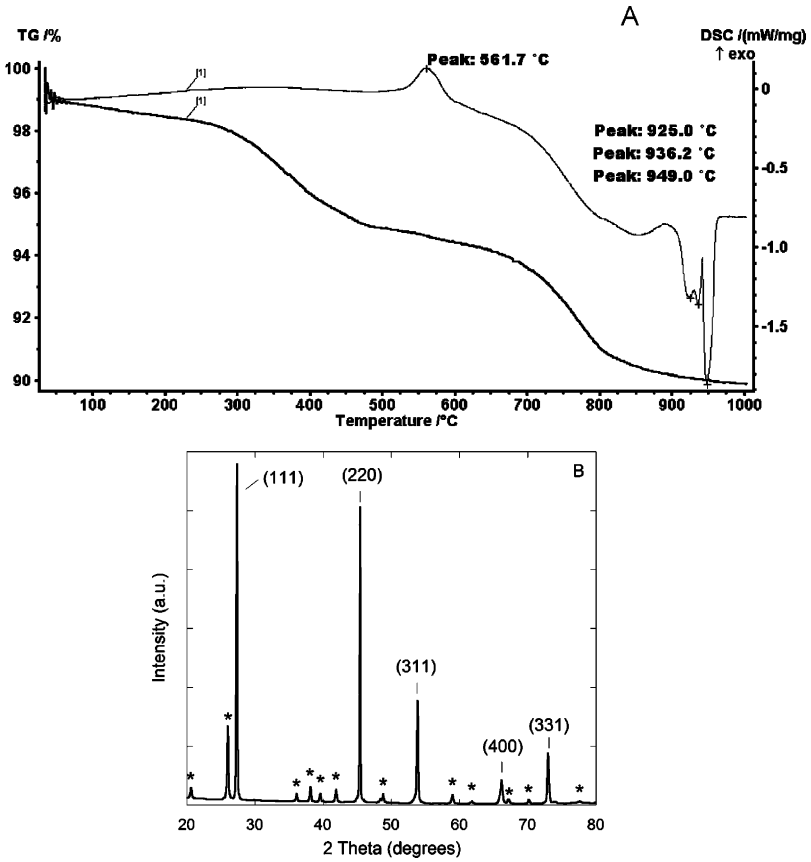

Figure 6. (A) Simultaneous TGA/DSC scans of Ge NPs preheated under vacuum to 400 °C. Data were collected on a 10 °C/min ramp rate under flowing argon. (B) Powder XRD pattern of the dry powder obtained after running TGA/DSC. The * peaks are due to germanium dioxide.

1.0 nm. TEM of this 600 °C material is consistent with well-dispersed Ge NPs with average size 7.6 ± 1.3 nm based on 391 particles and is very similar to the size obtained in XRD, 8.0 (1.0) nm. These results suggest that the NPs crystallize, but do not sinter, between 500 and 600 °C.

Figure 6A shows the TGA/DSC thermal analysis of a Ge NP sample that was heated to 400 °C under vacuum. This is a black solid that does not dissolve in any solvents. Elemental analysis provides the formula, $Ge(C_4H_9)_{0.15}$. There is an exothermic peak at approximate 561 °C, consistent with the onset of crystalline peaks in the XRD pattern attributed to Ge. A phase transition from amorphous to crystalline is an exothermic process. There is a very broad, nondistinct endotherm between 700 and 900 °C that may be associated with sintering of the NPs. There are distinct endothermic peaks at approximately 925, 936, and 949 °C. Bulk Ge is reported to melt at 937.4 °C.[30] The endotherms observed at 925−949 °C are consistent with melting of the NPs. Ge powder was also measured under the same conditions and showed a melting endotherm at 966 °C. The differences between this measurement and the literature value may be due to rate of heating and a mix of different phases of Ge in the sample. However, the slight reduction in melting for 8 nm Ge NPs is expected compared with bulk. The latent heat of crystallization can be extracted from the DSC data to be approximately 45.55 J/g. The latent heat of melting was calculated to be approximately 159.8 J/g and is about 3 times larger than the crystallization. From the TG data, about 2% weight loss was observed below 300 °C, then another 4% until 600 °C, and finally a weight loss of an additional 4% occurred around 800 °C, giving a total of 10%. The 10% loss corresponds well to the amount of hydrocarbon in the sample. Figure 6B shows the powder XRD pattern of the sample obtained after the TGA/DSC study. The major diffraction peaks can be assigned to crystalline Ge, and the smaller ones indicated with the symbol * are attributed to germanium dioxide.

From the in situ XRD patterns, it can be observed that the sample crystallizes in the diamond structure between 500 and 600 °C. In the as-prepared sample, the mean size was 4.5 ± 1.1 nm and shows crystallinity according to electron microscopy measurements. XRD was performed on the as-prepared sample, an orange oil; however, no diffraction by X-rays was observed. This is attributed to the small amount of NPs dispersed in a polymeric material. Even if all the Ge in the as-prepared sample is due to the NPs, there is only approximately 35 wt % Ge. As the sample was heated under vacuum to different temperatures, the average diameter of the particle increase and the 300 °C sample showed no electron diffraction and broad amorphous X-ray powder diffraction pattern.[24,25,31] The mean particle diameter was 5.1 ± 1.0 nm. The 450 °C sample also shows a broad diffraction pattern and a mean particle diameter of 6.0 ± 1.1 nm. At 600 °C the particles size was 7.6 ± 1.3 nm and the X-ray

(30) Weast, R. C. *CRC Handbook of Chemistry and Physics*, 1st student ed.; CRC Press: Boca Raton, FL, 1988.

(31) Tatsumi, Y.; Honda, H.; Ikegami, K.; Naito, S. *J. Phys. Soc. Jpn.* **1987**, *56*, 2977−2981.

powder diffraction pattern shows crystalline Ge. The DSC measurements show an exothermic peak consistent with the phase change from amorphous to crystalline Ge. The exotherm occurs concurrently with a weight loss. This might be due to removal of the hydrocarbon from the surface; however, this temperature is higher than expected based on bond energies. The Ge−C bond should break at approximately 245 °C based on the Ge−C bond strength.[32] Thermodynamic data on amorphous Ge suggests that the amorphous to crystalline temperature is at 692 °C.[33] This is the closest bulk phase transition analogous to the transition that is observed in these NPs. The lower transition temperature may be due to the concurrent loss of hydrocarbon from the surface. It is also possible that lower transition is characteristic of this diameter of Ge NPs. If that is the case, the temperature would be dependent on size and further experiments are necessary to determine this.

Size analysis of each sample provided above suggests that the NPs grow. This would be consistent with the presence of small Ge NPs or a high boiling point organo-germanium polymer providing a source of Ge. To remove ambiguities caused by slightly different sized NPs from different reactions, TEM data were collected on the as-prepared sample and the same sample was heated to 600 °C under vacuum. The as-prepared sample had an average diameter of 5 nm and the NPs obtained after heating were approximately 8 nm. These results suggest that the NPs grow, presumably by an Ostwald-type process, and imply that there is a source of Ge that contributes to this growth.

There have been some theoretical calculations on the structure and stability of small (1−2.5 nm) Ge NPs.[34] This energy calculation showed that, over a wide temperature range, cubic diamond Ge clusters are more stable than tetragonal-like structure observed in amorphous Ge. However, the energy difference between diamond structure and tetragonal-like structures was found to be strongly dependent on the structure and termination of the surface. The experiments presented herein suggest that there is a small energy difference between the diamond structure and the tetragonal-like amorphous structure of Ge, at least for NPs 4 nm and larger. A small amount of heat is enough to change the diamond structured as-prepared NPs into amorphous NPs (300 °C) and then a small exotherm is observed concurrent with the transition from amorphous back to crystalline NPs. Further studies with various diameter NPs with different surface termination are important to obtain a more complete thermodynamic picture of organically terminated Ge NPs.

Summary

A room-temperature solution reduction route can prepare crystalline Ge NPs. The reaction of $GeCl_4$ with Na(naphth) also produces an organic polymeric side product that contains Ge. The polymeric side product can be removed at 300 °C in vacuo. The approximately 4 nm diameter Ge NPs become amorphous and grow in size when heated under vacuum from 300 to 550 °C. There is a phase change at 561 °C from amorphous to crystalline NPs and an initial melting of 8 nm particles at 925 °C with subsequent melting to bulk Ge.

Acknowledgment. We thank Richard Baldwin for his early contribution to this work, acknowledge Ram Seshadri, Donna Senft, Giulia Galli, and Rajiv J. Berry for useful discussion, and Alexandra Navrotsky for the use of the TGA/DSC. Funding from AFOSR, NSF DMR-0120990, and CHE-0304871 is gratefully acknowledged.

Supporting Information Available: A figure of DSC scans of Ge NPs and bulk Ge (PDF). This material is available free of charge via the Internet at http://pubs.acs.org.

CM050674E

(32) Kerr, J. A. *CRC Handbook of Chemistry and Physics 1999−2000: A Ready-Reference Book of Chemical and Physical Data CRC Handbook of Chemistry and Physics*, 81st ed.; CRC Press: Boca Raton, FL, 2000.
(33) Donovan, E. P.; Spaepen, F.; Turnbull, D.; Poate, J. M.; Jacobson, D. C. *J. Appl. Phys.* **1985**, *57*, 1795−1804.
(34) Pizzagalli, L.; Galli, G.; Klepeis, J. E.; Gygi, F. *Phys. Rev. B: Condens. Matter* **2001**, *63*, 165324.